Applied Physics B: Lasers and Optics manuscript No.
(will be inserted by the editor)

A novel concept for in situ gas-phase laser Raman spectroscopy for solid oxide fuel cell research

G. Schiller[1], C. Auer[1], W.G. Bessler[1,3], C. Christenn[1], Z. Ilhan[1], P. Szabo[1], H. Ax[2], B. Kapadia[2], W. Meier[2]

German Aerospace Center (DLR), D-70569 Stuttgart, Germany
[1]Institute of Technical Thermodynamics, [2]Institute of Combustion Technology
[3]Universität Stuttgart, Institut für Thermodynamik und Wärmetechnik, D-70569 Stuttgart, Germany

Corresponding author:
Günter Schiller
E-Mail: guenter.schiller@dlr.de
Phone: +49 711 6862635

Abstract A planar solid oxide fuel cell (SOFC) operated with hydrogen at T=1123 K was equipped with an optically transparent anode flow field to apply species concentration measurements by 1D laser Raman scattering. The flow channels had a cross section of 3 mm × 4 mm and a length of 40 mm. The beam from a pulsed high-power frequency-doubled Nd:YAG laser (λ=532 nm) was directed through one channel and the Raman scattered light from different molecular species was imaged onto an intensified CCD camera. The main goal of the study was an assessment of the potential of this experimental configuration for a quantitative determination of local gas concentrations. The paper describes the configuration of the optically accessible SOFC, the laser system and optical setup for 1D Raman spectroscopy as well as the challenges associated with the measurements. Important aspects like laser pulse shaping, signal background and signal quality are addressed. Examples of measured species concentration profiles are presented.

1. Introduction

Solid oxide fuel cells (SOFC) are highly efficient converters of chemical energy from fuels into electrical energy considered for a future environmentally friendly energy supply. High electrical performance and long lifetime are key requirements that must be fulfilled for a successful introduction into the market. Inhomogeneous distributions of electrochemical and thermal properties such as local

power density and local temperature can detrimentally affect both efficiency and long-term durability through thermo-mechanical stress and degradation phenomena induced by locally varying operating conditions [1]. The application of advanced diagnostic methods for monitoring cell characteristics of solid oxide fuel cells under real operating conditions can provide detailed information about the spatial distribution of cell properties in order to increase the fundamental understanding and to optimize the operational behavior.

Electrochemical diagnostics (polarization curves, electrochemical impedance spectra) is playing a major role in fuel cell investigations. To study inhomogeneous cell properties during operation, we have previously extended traditional methods and have developed spatially resolved diagnostic techniques such as segmented cell technology that allows for the in situ determination of local current density and voltage, local impedance data, and temperature distribution as well as local gas concentrations [2,3,4]. The obtained data can be used for mathematical modeling and model validation and for predicting physical, electrochemical and fluid mechanical properties [5].

To complement the existing diagnostic techniques, advanced laser measurement techniques can be adopted. They allow a spatially and temporally resolved in-situ determination of gas-phase properties such as composition, temperature and flow velocity [6]. In this work, we develop and demonstrate a diagnostic method based on gas-phase Raman laser scattering. Gas-phase Raman spectroscopy in the flow channel of an SOFC has recently been reported by Saunders and Davy [7]. Their optically accessible SOFC and Raman setup was quite different from the one described here. For example, their reformer channel was significantly larger, they used a broadband XeCl excimer laser (λ=308 nm) and their setup did not allow for a 1D measurement along the flow direction. Solid-state Raman spectroscopy has been applied for studying SOFC processes ex-situ [8-11] but these studies were mainly devoted to the measurement of local temperature and mapping out of phase stability of solid electrode surfaces by monitoring the temporal variation of the oxidation state of materials. Tunable diode laser absorption spectroscopy in the near-infrared has been applied to analyze water vapor and methane concentrations in a solid oxide fuel cell [12]. A combination of ex situ Fourier Transform Infrared Spectroscopy (FTIR), in situ Raman spectroscopy and Electrochemical Impedance Spectroscopy (EIS) measurements was used to study carbon formation and deposition on anode surface [13] as well as sulfur poisoning mechanisms, CO oxidation and NiO redox kinetics [14].

Spontaneous Raman scattering is widely used in chemical analysis and related areas for species measurements [15]. Due to the inherently small scattering cross section, Raman spectroscopy of gaseous species requires powerful lasers for excitation as well as efficient detection schemes. Meier et al. [16] and Stricker [17] have been extensively employing laser Raman scattering for species and temperature measurements in flames using pulsed high-power lasers. Since spontaneous Raman

scattering is a non-resonant process, it allows for the simultaneous detection of multiple molecular species, which can be distinguished by their different Raman shifts (vibrational energy quant in case of vibrational Raman scattering). In a 1D configuration, spatial measurement resolution can be achieved for multi-species Raman measurements in the direction along the laser beam by employing a detection scheme with a spectrograph in combination with a CCD camera [17]. Such a setup was employed in the current investigation where a narrow high-power laser beam (λ=532 nm) was directed through one of the anode flow channels of the SOFC in flow direction and the scattered light was detected at 90°. This enabled the detection of the species concentration profiles along the flow direction. In the current investigation, the SOFC was fuelled with hydrogen. Thus, the only major species present during the operation were H_2 and H_2O (and N_2 after the occurrence of a leak). The corresponding Raman signals could be well separated and yielded sufficient signal-to-noise ratio for a quantitative evaluation after averaging single-shot Raman spectra.

The work described in this paper demonstrates our experimental approach for a better understanding of the processes within the anode flow channel. The main focus lies on the description of the optical cell, the electrochemical test bench and the Raman measurement setup as well as the discussion of the performance of the system. First results of in situ measurements of anode gas concentrations measured simultaneously in one dimension along the flow channel are reported.

2. Challenges in operating an optically accessible SOFC

A number of challenges are encountered in operating an optically accessible SOFC at about 1123 K and performing gas-phase Raman spectroscopy in it. Requirement for laser-based techniques is optical access both for the laser beam itself and the laser-induced optical signals. This is not trivial in case of the complex geometry and high operating temperatures (800-1000 °C) of SOFCs, which are usually based on opaque ceramic materials. Therefore, an important step towards the applicability of laser diagnostics lies in the construction of SOFCs with optical access which are able to operate under technically relevant conditions. In the work described here, an optically transparent anode flow field for a planar SOFC cell is applied which allows for the investigation of the concentrations of relevant gaseous species within the anode flow channel. The SOFC and the test rig have been designed for the application of one-dimensional laser Raman spectroscopy. With respect to the SOFC, a construction enabling a leak-tight operation of the cell and coping with fouling of the quartz glass surfaces are issues. The experimental setup is described in more detail in the following section 3.1.

As for the 1D Raman measurement setup, the collimation of a high-power laser beam to a long and narrow beam waist (over 40 mm length) without damaging the glass or generating an optical breakdown (plasma) presents a trade-off between signal strength and damage. It is also difficult to

maintain the alignment of the laser beam during the heat-up phase of the fuel cell setup. Signal background arising from Rayleigh scattering and laser stray light from surfaces must be efficiently reduced by proper beam alignment and optical filters. Another source of signal background is laser-induced luminescence from quartz glass that interferes with the Raman signals. For the conversion of the Raman signals to species mole fractions, calibration measurements are necessary which should be performed under the same optical boundary conditions as the measurements in the operating fuel cell. Great care has to be taken to maintain the boundary conditions (like optical alignment or window transmissivity) during the measurements. These aspects were addressed in the present work.

3. Experimental setup

3.1 SOFC test station

A SOFC test station from FuelCon, Magdeburg, Barleben, Germany (Type Evaluator C100-HT) including a customized furnace with a maximum temperature of 1100 °C was equipped with ports (10x50 mm^2) for the laser beam and a quartz glass window (150 mm diameter) for the detection of the Raman signals. Fig. 1 shows a photograph of the opened furnace during laser test operation. The furnace confines a cylindrical volume of 300 mm diameter in which the SOFC cell was placed. For the installation of the cell and laser alignment, the upper part of the furnace could be opened. A sketch of the experimental arrangement in Fig. 2 illustrates the experimental setup with a view from side and top.

The setup for the cell compartment is based on a non-standard ceramic housing. A schematic drawing of the cell housing is shown in Fig. 3. The cell was placed in upright position between an anode (quartz) and a cathode (alumina) flow field in an alumina housing and sealed by gold rings. The pressure for sealing was applied via a ceramic wedge with a weight (2 kg) on its top. For contacting, platinum nets were used on both the anode and the cathode side. Fig. 4 shows a photograph of the SOFC setup taken through the observation window of the furnace during operation at high temperature. Planar electrolyte-supported cells (ESC) were used for the measurements. Cells with a size of 50x50 mm^2 were obtained from H.C. Starck Ceramics (Selb, Germany). They consisted of a Ni/GDC anode (40 µm), a TZ3Y electrolyte (100 µm) and a 8YSZ/LSM-LSM cathode (40 µm). ESCs have advantages for this type of test setup since it is possible to seal both gas manifolds with gold rings and the 100 µm thick, leak tight electrolyte enables a good electrochemistry.

In order to provide optical access to the anode of the cell the anode flow field was entirely consisting of polished quartz glass (Suprasil 2 grade B) and hence transparent in the spectral range of interest. A cut-out along a gas channel was introduced in the Pt contact mesh in order to ensure visibility to the anode layer for the Raman spectroscopy. The complex flow field with 9 narrow channels (2×2 mm^2 in the first

setup, 3×4 mm^2 in the setup reported here) and a length of 40 mm has been fabricated using a thermal bonding technique for glass material (Hellma, Müllheim, Germany). Fig. 5 shows a photograph of the transparent flow field for the anode. The SOFC cell could be supplied by different fuel gases (H_2, N_2, H_2O, CH_4, CO, CO_2) and air; a system software (FuelWork) managed all test parameters, provided data logging and controlled a multistage alarm system with sensors for hydrogen and CO. The gases for cell operation were supplied by tubes made of Inconel.

3.2 Background on laser Raman scattering

Spontaneous Raman scattering is based on the interaction between light and polarizable molecules. In the case of vibrational Raman scattering, which is considered here, the wavelength of the scattered light is shifted compared to the exciting laser wavelength by an amount that corresponds to the vibrational energy quantum of the molecule. Thus, different molecular species within a probe can be distinguished by analyzing the spectral composition of the scattered light. Furthermore, the species number density can be deduced from the intensity of the Raman-scattered light at the corresponding wavelength. The scattered intensity is proportional to the number density, the scattering cross section, the laser intensity, the size of the measurement volume, and depends on the detection arrangement and efficiency [6]. If the Raman-scattered radiation from each species i within the probe is detected and analyzed, all species number densities n_i are known and the sum of them yields the total number density $n=\Sigma n_i$. With the knowledge of the pressure p, the temperature T is then given by the ideal gas law, $T=p/(n\cdot k)$, where k is the Boltzmann constant. The goal of a Raman measurement for analyzing a gas composition lies in the simultaneous determination of all species number densities which then yields the corresponding mole fractions X_i and the temperature T [6, 19].

The Raman scattering cross sections are small and in order to achieve sufficient signal intensities, a high-power laser and an efficient detection system are needed. However, even excellent equipment enables only the detection of the major species with mole fractions larger than $X\approx0.005$. The biggest challenge of applying laser Raman scattering in reacting flows is to obtain a sufficient signal-to-noise (S/N) ratio. In order to reduce signal background from ambient light and detector noise, it is common in Raman measurements of reactive flows to use pulsed high power lasers and limit the detection gate to the pulse duration of the laser. However, due to the short pulse durations of these lasers of typically $\tau\approx10$ ns, small laser beam diameters generate high power densities that easily lead to optical breakdown (plasma generation) or damage of optical elements in the beam path. Therefore, these systems are mostly equipped with pulse stretchers. For the quantitative evaluation of the Raman signals, calibration measurements in flows of well-defined composition and temperature are needed.

3.3 Laser Raman setup

The optical setup is shown schematically in Fig. 6. The laser system consisted of three double-pulse Nd:YAG lasers (Spectra-Physics PIV 400), which generated a beam consisting of six frequency-doubled pulses (λ = 532 nm). After passing through a pulse stretcher, the combined pulse had a duration of $\tau \approx 350$ ns and a pulse energy of $E_p \approx 1.2$ J. This laser system is usually employed for Raman measurements in flames and is described in more detail in the literature [20, 21]. The laser beam had to be shaped to pass through the 40 mm long anode gas channel, cross section 3×4 mm^2, of the SOFC without damaging the transparent flow field section and without generating considerable amounts of stray light or luminescent emissions in the quartz glass. Therefore, the laser beam was focused by a spherical lens (f=3 m) in a way that the beam had a waist of approximately 2 mm in the transparent flow field. To avoid damage of the flow field section, the laser pulse energy was reduced to $E_p \approx 0.1$ J by means of a combination of a λ/2 wave plate and a Glan polarizer (see Fig. 6). The laser pulse energy was monitored in front of and behind the furnace. This enabled a control of the alignment and transmission of the setup and a good estimation of the laser energy in the channel of the flow field.

The scattered light from the laser beam was collected at 90° by an achromatic lens (f=160 mm) and relayed to the entrance slit of a spectrograph (Acton Research SpectraPro 300i, f=300 mm, 490 lines/mm, f/4, dispersion ~6 nm/mm). The magnification of the detection optics was 0.4. The entrance slit had a length of 14 mm and the width was set to 0.5 mm. A holographic notch filter in front of the spectrograph blocked the Rayleigh scattered light and the stray light at 532 nm. The spectrally dispersed image of the light distribution in the entrance slit was captured by an intensified CCD camera (Princeton Instruments PI-Max, 1340×1300 pixels, 26.8 mm × 26 mm chip size) equipped with a fiber-coupled image intensifier (Gen III, GaAs photocathode). By applying an on-chip accumulation of the pixel intensities of several single exposures it was possible to lower the effect of readout noise. The raw data acquired by the 1D Raman system consisted of image files with a spatial resolution in the vertical and a spectral resolution in the horizontal direction. The imaged volume had a length of 35 mm and was divided by pixel binning into 35 superpixels in the spatial direction, corresponding to 35 measurement volumes each with a length of 1 mm and diameter of ~2 mm (according to the diameter of the laser beam in the observed section). The 35 spectra from these volumes were recorded simultaneously. In the spectral dimension, five adjacent pixels were binned to 268 superpixels with a spectral resolution of about 0.6 nm.

In order to reduce stray light and luminescence detection from the quartz surface of the channel, only the core region of the laser beam was imaged through the entrance slit and the periphery was clipped by the entrance slit (vignetting). Since the laser beam was not exactly parallel along the detected region,

the transmitted part varies along the imaged line. The corresponding variation in detection efficiency was measured before the final measurements by recording the Raman signal from pure hydrogen in the flow channel.

The quantitative data evaluation of these images was based on the comparison of the Raman signals from the fuel cell with signals from the calibration measurement. The pre-processing of the data included several image processing steps (spectral shift correction, background subtraction, intensity normalizations to laser pulse energy and intensifier gain, correction for vignetting). The species-specific Raman bands were integrated over a spectral range (also termed Raman channels). Due to the given spectral resolution, Raman bands from different species can spectrally overlap. This crosstalk was measured in the calibration measurements and incorporated into the data evaluation routine. After the pre-processing and crosstalk corrections, the intensities of the different Raman channels are converted to absolute number densities (or mole fractions).

3.4 Raman calibration measurements

In combustion experiments the calibration of the Raman system is performed in cold and electrically heated gas flows and laminar flames of known temperature and gas composition. Because the Raman cross sections and the shapes of the Raman bands as well as the overlap between adjacent Raman bands are temperature dependent, calibration measurements for flame investigations must be performed at temperatures covering a wide range. The post-processing procedure turning Raman signals into concentrations is usually based on a matrix inversion method [22]. In the current experiment the effort was less because the temperature of the anode flow was the same as that of the furnace and was continuously measured during operation by thermocouples. The only species present in the flow channel were H_2 and H_2O, because only hydrogen was used as fuel. The crosstalk between these species was so small that it could be neglected. The signal from hydrogen was calibrated by passing pure H_2 through the channel with the fuel cell at open cell voltage. Calibration for water was not performed because it was difficult to fill the flow channel with a defined concentration of H_2O. However, with only H_2 and H_2O present, their mole fractions had to add up to 1 so that an individual calibration for H_2O was not necessary.

4. Results

4.1 Initial optical signal characterization

Initial laser measurements revealed a broadband background signal that could be attributed to laser-induced luminescence of the quartz flow field. In order to determine the spectral composition and

intensity distribution of this luminescence under the current experimental conditions, a glass block with the dimension 10 mm × 10 mm × 40 mm, made of the same quartz material as the transparent flow field, was installed in the measurement location and irradiated with the laser light. Figure 7 shows the spectrum recorded at 300 K. The spectral region around the laser wavelength that was blocked by the notch filter is indicated by the hatched area. The luminescence exhibited distinct spectral signatures with the strongest emissions close to the laser wavelength and rapidly decreasing intensities at longer wavelengths. The wavelength positions of the Raman bands of some relevant species are also indicated. The strongest disturbance is expected for CO_2 which is, however, not present in the current measurements. At an elevated temperature of 1123 K the signal intensity of the luminescence emission has significantly dropped (see Fig. 8). For the CO_2 Raman channel, the interference still poses a problem, however, for the other species the interferences are manageable. The signal background from these emissions was scaled and subtracted from the Raman spectra obtained from measurements during fuel cell operation.

Fig. 9 displays Raman spectra of room air measured within the flow channel. Each of the 35 spectra corresponds to one segment of 1 mm length along the imaged length along the laser. Here, 200 single laser shot signals were accumulated and corrected for background. The different detection efficiencies along the spatial direction were not corrected for in this image. The strongest line at $\lambda \approx 608$ nm represents N_2, the line at $\lambda \approx 582$ nm O_2. Also seen is the Raman signal from H_2O at $\lambda \approx 662$ nm from the humidity of the air. The air composition and temperature within the flow channel was constant and the different signal intensities seen in the Raman spectra are caused by a varying sensitivity of the camera chip and the fact that a part of the Raman-scattered light is clipped by the entrance slit of the spectrograph.

4.2 Initial SOFC operation

Operation of a solid oxide fuel cell requires a specific start-up protocol which was chosen as follows. A fresh SOFC was heated to approximately 1123 K under supply of 0.25 standard liter per minute (slpm) of forming gas (5% H_2 in N_2) to the anode and 0.25 slpm of air to the cathode. After the cell was heated up to the target temperature the anode was reduced, that is, nickel oxide (NiO) present in the anode after cell manufacturing was converted to Ni, the active electrocatalyst. This was achieved by gradually increasing the fuel flow of hydrogen to the anode to 1.25 slpm and the air flow to the cathode to 1.25 slpm. The forming gas was reduced to 0 slpm. The reduction process lasted about 1 h and yielded an open circuit voltage (OCV) of 1.209 V. Subsequently, a polarization curve was recorded by increasing the current load on the cell until the cell voltage reached a lower limit of 0.6 V. The results are shown in Fig. 10. At a voltage of 0.7 V the power density of the cell reached 340 mW/cm². For this cell type the

value is quite high indicating that the cell setup was gas-tight. At a lower fuel gas flow of 0.112 slpm the cell still produced a power density of 219 mW/cm².

The system was kept at high temperature for the period of the measurements of 15 days. The ceramic parts of the furnace were red hot at this temperature and excluded a close inspection of the quartz cell by eye (see Figure 4). During the course of the measurement period, the optical transmission of the transparent part of the cell housing and also that of the observation window of the furnace degraded due to a greyish deposit whose origin could not unambiguously be identified. The corresponding reduction in transmission reduced the signal intensity and was taken into account in the data reduction routine.

4.3 Raman laser diagnostics under SOFC operation

In-situ Raman laser diagnostics was carried out during SOFC operation under a range of different conditions. Here we present exemplary results for 1123 K, dry H_2 as anode gas (1.25 slpm) and air at the cathode (1.25 slpm) for different currents between 0 and 7 A (corresponding to current densities of 0 – 437.5 mA/cm^2). For each operating point, the Raman signals from 3000 laser shots were accumulated on-chip (corresponding to about 5 minutes measuring time) and corrected for background, vignetting, varying detection efficiency and laser pulse energy. Fig. 11 shows Raman spectra recorded at 312.5 mA/cm^2. The 35 spectra cover a length of 35 mm along the channel. The H_2O Raman band appears at $\lambda \approx 660$ nm and the H_2 Raman band at $\lambda \approx 683$ nm. The H_2 signal decreases along the fuel flow direction (from back to front in the figure) while the H_2O signal increases. Thus, the anodic fuel cell reaction,

$$H_2 + O^{2-} \rightleftarrows H_2O + 2\,e^- \quad ,$$

could be successfully monitored in situ with high spatial resolution (1 mm) at realistic operating conditions.

Gas-phase concentrations are proportional to the area under the Raman signals. Therefore, relative concentrations were determined from the Raman spectra shown in Fig. 11. Resulting concentration profiles along the length of the channel are shown in Fig. 12 for various current densities. At open circuit voltage (OCV) without any electrochemical reaction the relative concentrations of H_2 and H_2O are constant along the flow channel. The apparent slight decrease of the H_2 profile is most likely due to uncertainties related to the signal correction procedure. Under load (1-7 A) the hydrogen concentrations decrease and the steam concentrations increase along the channel length as is expected with ongoing electrochemical reactions.

The quality of the Raman signals is sufficient for a quantitative data analysis. However, during the measurement period a leakage in the sealing of the cell appeared which was noticed through the

appearance of N_2 signals in the Raman spectra. This leakage resulted in the uncontrolled chemical oxidation of hydrogen to steam even at OCV conditions so that a quantitative evaluation of the obtained Raman signals was no longer possible.

5. Discussion

With respect to the Raman measurements, the optical arrangement with the laser beam passing through the channel and signal detection at 90° enabled the observation of the concentration profiles along the channel without moving parts of the setup to change the measurement location. This geometry is different from the one applied in a previous setup [7] and proved to be convenient in our experiment. The difficulties related to this setup are the generation of a long narrow laser beam waist and the avoidance of an optical breakdown and/or damage of the transparent flow by too high laser fluence. In the current setup, the laser pulse energy was reduced to 0.1 J in order to be clearly below the damage threshold. This corresponds to an average laser power of approximately 286 kW over the 350 ns long pulse duration which is still orders of magnitude larger than the power of CW lasers. A further stretching of the laser pulse would allow to couple more laser pulse energy into the cell and to increase the signal level. It is noted that the pulse duration of a "standard" flashlamp-pumped Nd:YAG is in the order of 10 ns. Applying a similar laser power from such a laser, the pulse energy must be reduced to $E_p \approx 0.003$ J which is certainly too low for Raman spectroscopy in this application. Care must also be taken to avoid significant generation of laser-induced luminescence from the quartz glass. Due to the small cross section of the channel and the inhomogeneous laser beam profile, exposure of the channel walls to the laser radiation cannot be completely avoided. The analysis of the luminescence signal showed that the problems are less pronounced at elevated temperatures compared to room temperature, but that they might require a more comprehensive background correction for the detection of the CO_2 Raman band. Aside from this difficulty, the Raman scattering technique can also be applied using fuels other than hydrogen in this configuration, e.g. methane. In that case, the calibration would include CH_4, CO, and CO_2 passing through the channel with the fuel cell at open cell voltage. The crosstalk corrections would be similar to those applied in flame investigations.

In the current setup the signal-to-noise ratio was sufficient for quantitative measurements. However, due to the leakage through a crevice in the assembled cell the results presented here could not be given in mole fractions. At this stage, single shot Raman measurements are hardly quantifiable because they do not yield sufficient signal-to-noise ratio. However, the temporal changes within the SOFC are slow enabling an accumulation of Raman signals over several minutes. Also, a spatial resolution of 1 mm as applied here seems unnecessary and a further binning of pixels would lead to a better signal quality.

Quantitative results of gas concentration measurement by in situ Raman spectroscopy within an operating SOFC can only be achieved when the cell is properly sealed against the surrounding gas atmosphere. This sealing represents a major challenge in the SOFC setup used. A proper sealing which is realized by gold rings, however, requires sufficient pressure which can only be applied in horizontal direction in the cell setup used. This means that all parts must ideally fit during the cell assembly process. In order to assure improved sealing conditions, constructional modifications of the cell compartment and a modified sealing are under development for the future investigations. When achieving a properly operating SOFC Raman measurements will be performed by applying various operating conditions including complex fuel gas compositions, such as different reformate compositions, and temperature and flow rate variations. The obtained data will be particularly useful for validating detailed models of reforming and fuel cell processes using a physically-based modelling framework developed by Bessler et al. [23].

Summary and Conclusions

A novel experimental approach was presented for the analysis of chemical species conversion within a solid oxide fuel cell (SOFC) flow channel, based on gas-phase laser diagnostics. The complete anode flow field was made out of fused silica enabling access for optical measurement techniques. The transparent SOFC was installed into a test bench with window equipped furnace allowing in-situ optical access at temperatures up to 1273 K and SOFC operation under various fuel compositions. For the measurement of species concentration profiles, one-dimensional laser Raman scattering was applied. The pulse train from 3 double pulse Nd:YAG lasers was extended in a pulse stretcher to a total duration of approximately 350 ns and focussed into one of the 3×4 mm^2 wide flow channels. The pulse energy was reduced to $E_p \approx 0.1$ J in order to prevent optical breakdown or damage of the transparent cell component. The relatively long pulse duration was necessary to introduce sufficient laser energy into the flow channel. The setup enabled the detection of the species concentration profiles along a line of 35 mm length within the 40 mm long flow channel.

A number of initial experiments were performed in order to characterize and validate the measurement technique. This included identification of background signals and calibration measurements. When the flow channel was filled with cold air, the Raman bands of N_2, O_2 and residual H_2O were well resolved. The technique was then successfully applied for in-situ diagnostics of a SOFC operating under standard conditions of 1123 K and dry hydrogen. Under these conditions the Raman bands of H_2 and H_2O were detected and yielded sufficient signal-to-noise ratio for a quantitative evaluation after an accumulation of 3000 laser shots. The profiles were recorded with a spatial resolution of 1 mm along the channel length and exhibited clearly the expected behaviour, i.e. a decrease of H_2 and increase of H_2O

concentration along the flow direction. However, due to a leakage of the cell the concentrations could not be quantified.

The results demonstrated the feasibility of measuring species concentration profiles by laser Raman spectroscopy in this arrangement. In the next step, an improved cell setup will be used to perform quantitative species measurements at various operating conditions. As Raman scattering allows the simultaneous detection and distinction of different gas-phase species, this technique will be particularly useful for investigating internal reforming conditions where CH_4, H_2, H_2O, CO, CO_2 and N_2 are present simultaneously.

Acknowledgement

Financial support from the Initiative and Networking Fund of the Helmholtz Association is gratefully acknowledged.

References

[1] P. Metzger, K.A. Friedrich, H. Müller-Steinhagen, G. Schiller, Solid State Ionics **177**, 2045-2051 (2006)

[2] P. Metzger, *Ortsaufgelöste Charakterisierung von Festelektrolyt-Brennstoffzellen (SOFC) durch Messung betriebsrelevanter Größen entlang des Strömungswegs*, PhD thesis, University of Stuttgart (2010)

[3] G. Schiller, W. Bessler, K.A. Friedrich S. Gewies, C. Willich, ECS Trans. **17**(1),79-87 (2009)

[4] P. Metzger, K.A. Friedrich G. Schiller, C. Willich, J. Fuel Cell Sci. Technol. **6**(2), 021304-1 – 021304-4 (2009)

[5] W.G. Bessler, S. Gewies, C. Willich, G. Schiller, K.A. Friedrich, Fuel Cells **10** (3), 411-418 (2010)

[6] A.C. Eckbreth, *Laser Diagnostics for Combustion Temperature and Species*, (Gordon & Breach, The Netherlands, 1996)

[7] J.E.A. Saunders, M.H. Davy, Int. J. Hydrogen Energy **37**, 3403-3414 (2012)

[8] R.C. Maher, L.F. Cohen, P. Lohsoontorn, D.J.L. Brett, N.P. Brandon, J. Phys. Chem. A **112**, 1497-1501 (2008)

[9] M.P. Pomfret, J.C. Owrutsky, R.A. Walker, J. Phys. Chem. B **110** (35), 17305-17308 (2006)

[10] M.P. Pomfret, J.C. Owrutsky, R.A. Walker, Anal. Chem. **79** (6), 2367-2372 (2007)

[11] Z. Cheng, M. Liu, Solid State Ionics **178**(13-14), 925-935 (2007)

[12] A.J. McGettrick, W. Johnstone, R. Cunningham, J.D. Black, J. Lightwave Technol. **27** (15), 3150-3161 (2009)

[13] B.C. Eigenbrodt, J.D. Kirtley, R.A. Walker, ECS Trans. **35**(1), 2789-2798, (2011)

[14] E. Brightman, R. Maher, D.G. Ivey, G. Offer, N. Brandon, ECS Trans. **35** (1), 1407-1419 (2011)

[15] M.J. Pelletier, *Analytical Applications of Raman Spectroscopy* (Wiley VCH, Weinheim, 1995)

[16] W. Meier, R.S. Barlow, Y.-L. Chen, J.-Y. Chen, Combust. Flame **123**, 326-343 (2000)

[17] W. Stricker in *Applied Combustion Diagnostics*, ed. by K. Kohse-Höinghaus, J. Jeffries, (Taylor and Francis, New York, 2002) pp. 155-193

[18] R.S. Barlow, Proc. Combust. Institute 31, 49-75 (2007)

[19] R.S. Barlow, C.D. Carter, R.W. Pitz, in *Applied Combustion Diagnostics*, ed. by K. Kohse-Höinghaus, J. Jeffries (Taylor & Francis, New York, 2002) pp. 384-407

[20] H. Ax, P. Kutne, W. Meier, K. König, U. Maas, A. Class, M. Aigner, Appl. Phys. B **94**, 705-714 (2009)

[21] U. Stopper, M. Aigner, H. Ax, W. Meier, R. Sadanandan, M. Stöhr, A. Bonaldo, Exp. Thermal Fluid Sci. **34**, 396–403 (2010)

[22] R.W. Dibble, S.H. Starner, A.R. Masri, R.S. Barlow, Appl. Phys. B **51**, 39-43 (1990)

[23] W.G. Bessler, S. Gewies, M. Vogler, Electrochimica Acta **53**, 1782-1800 (2007)

Figures

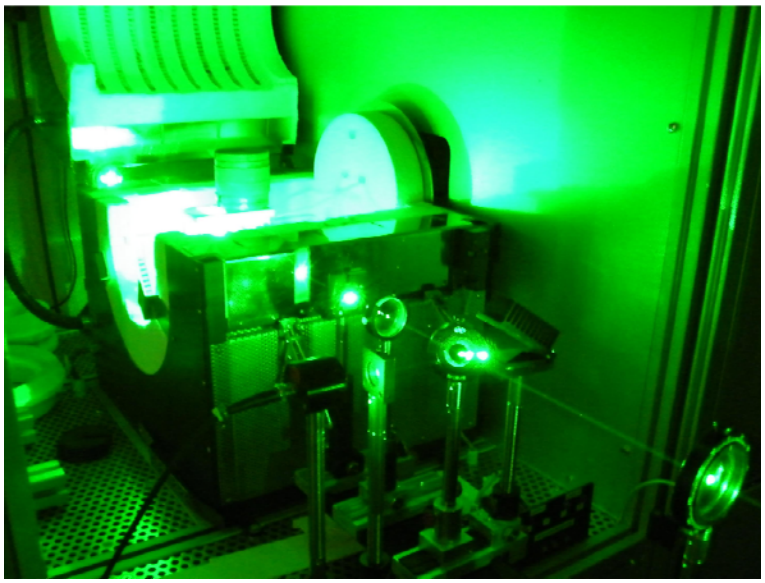

Fig. 1: Photograph of the furnace with opened cover and laser beam (λ=532 nm) traveling from the bottom right into the furnace. The Raman scattered light is collected perpendicularly to the laser beam through the opening on the left side. The photo also illustrates the huge amount of laser stray light from surfaces.

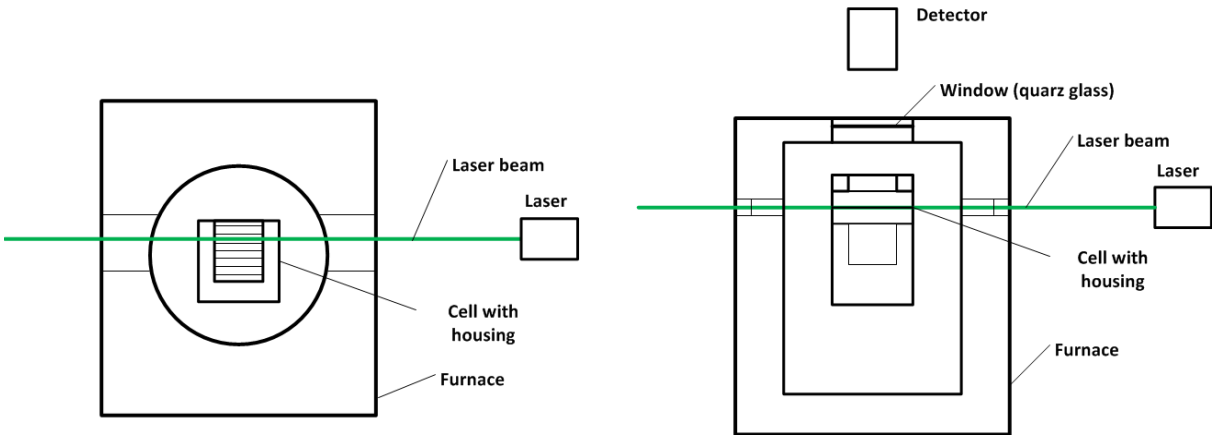

Fig. 2: Sketch of the experimental arrangement illustrating the experimental setup: side view (left), top view (right)

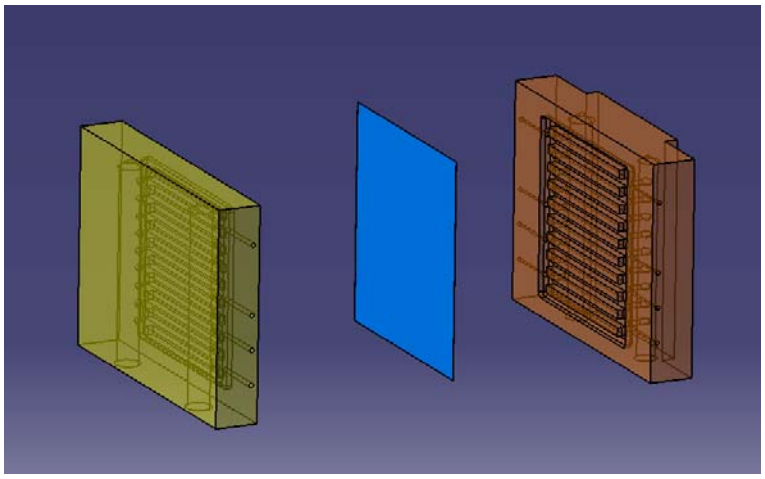

Fig. 3: View of cell test assembly with gas flow fields. The flow field for the anode gas (right) is transparent consisting of quartz glass, the flow field for the cathode gas (left) consists of alumina. The cell itself (middle) is placed between the two flow fields.

Fig. 4: Photo of the SOFC cell compartment through the observation window for the detection of the Raman scattered radiation. The furnace is at $T \approx 1123$ K. The central part is the transparent flow field consisting of quartz glass and surrounded by ceramic parts. The green line indicates the laser beam.

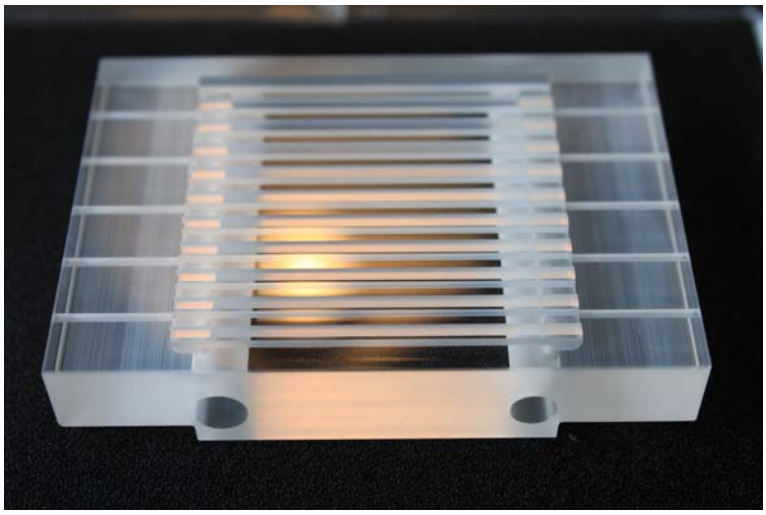

Fig. 5: Transparent anode flow field consisting of quartz glass with 9 gas channels (3x4 mm^2)

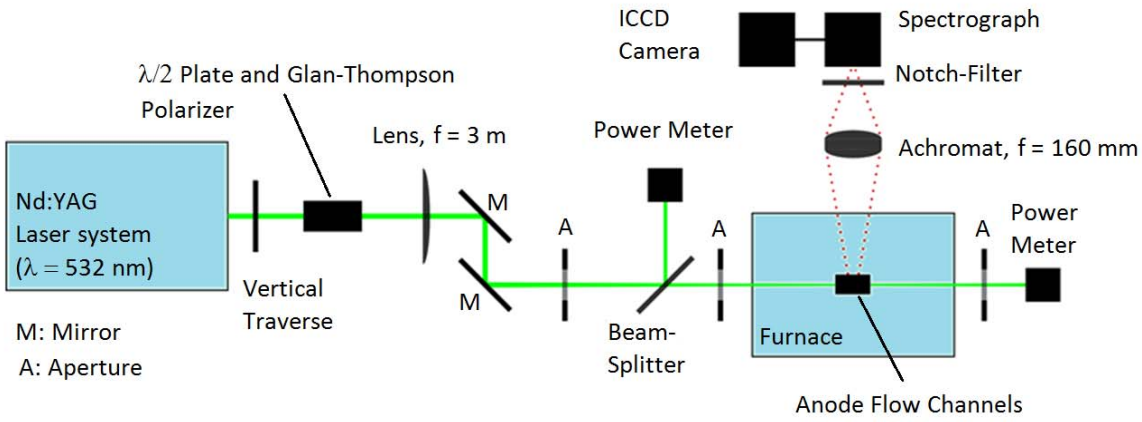

Fig. 6: Schematic of the experimental setup

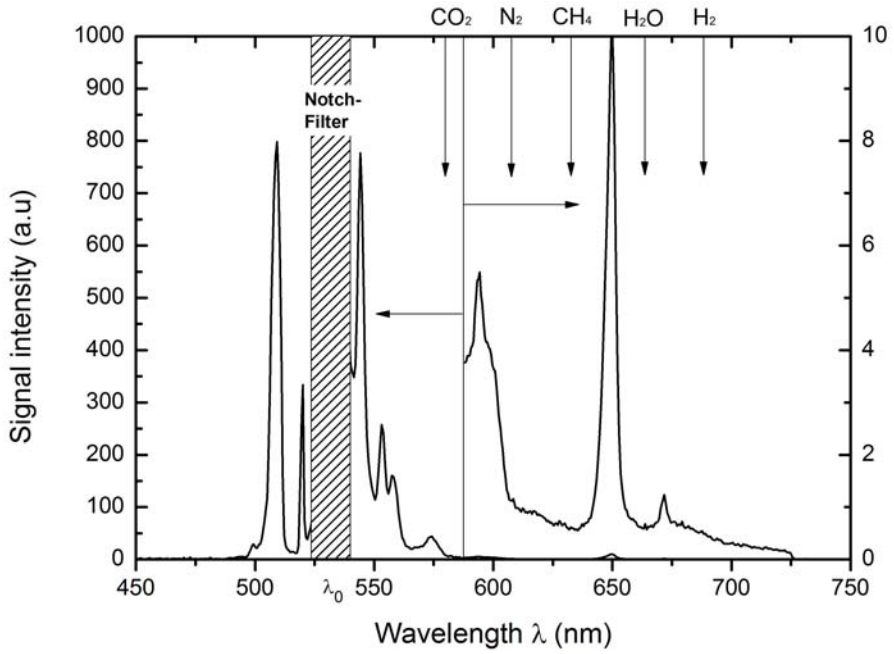

Fig. 7: Spectrum of the luminescence from quartz (Suprasil® 2 Grade B) at T=300 K after illumination with pulsed laser radiation at λ=532 nm. Note that the intensity scale is changed at λ≈585 nm. The hatched area was masked by the notch filter in front of the spectrograph. The vertical arrows indicate the positions of the Raman bands of different species.

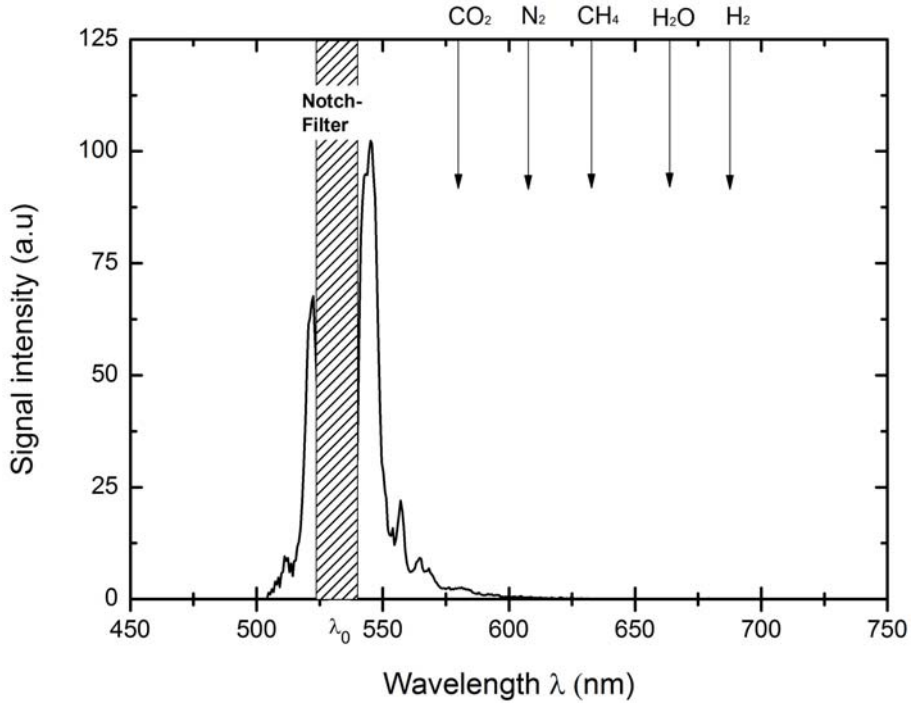

Fig. 8: Spectrum of the luminescence from quartz at T=1123 K after illumination with pulsed laser radiation at λ=532 nm. The signal intensity is scaled to the level of Fig. 7.

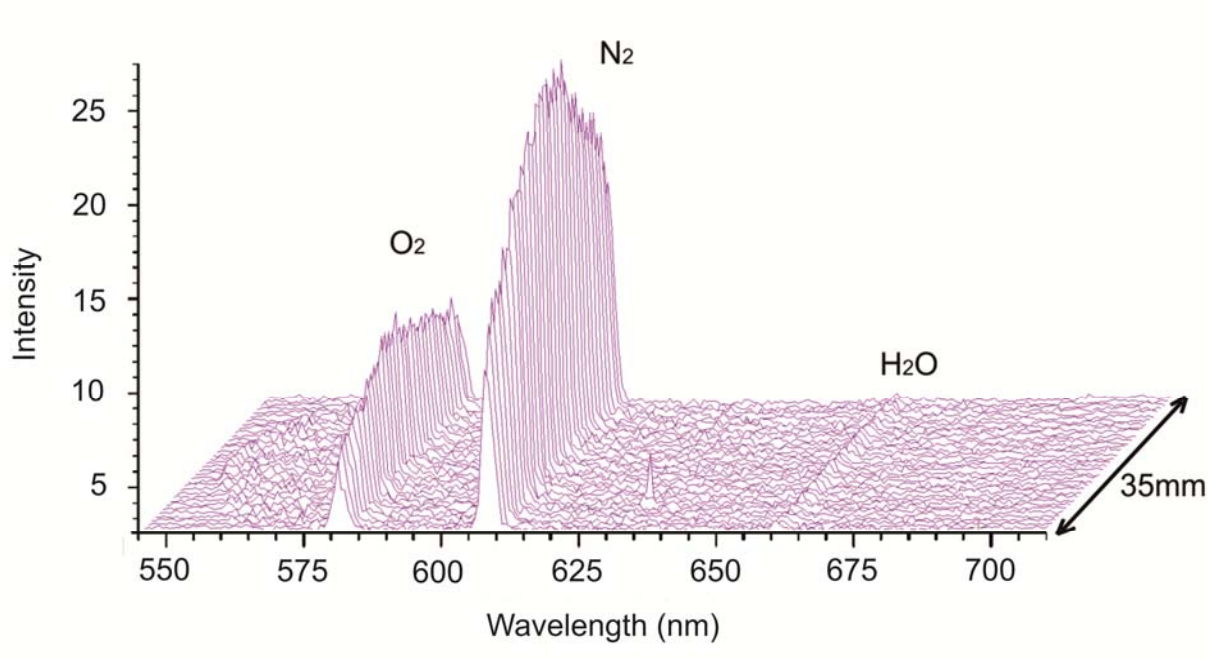

Fig. 9: Raman spectra of room air measured within the flow channel. Each of the 35 spectra corresponds to one segment of 1 mm length along the imaged length along the laser. 200 laser shots were accumulated.

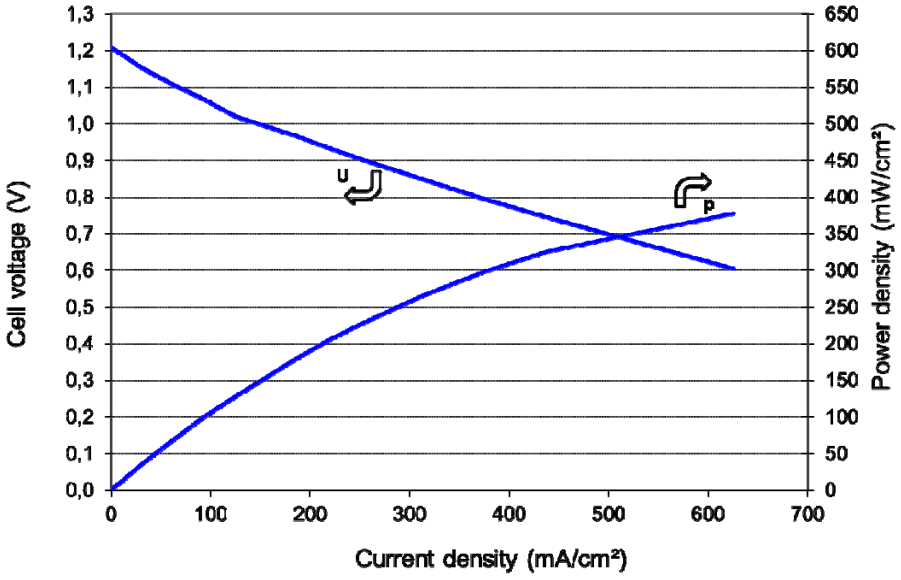

Fig. 10: Polarization curve of solid oxide fuel cell (16 cm^2 active cell area) operated at 1123 K

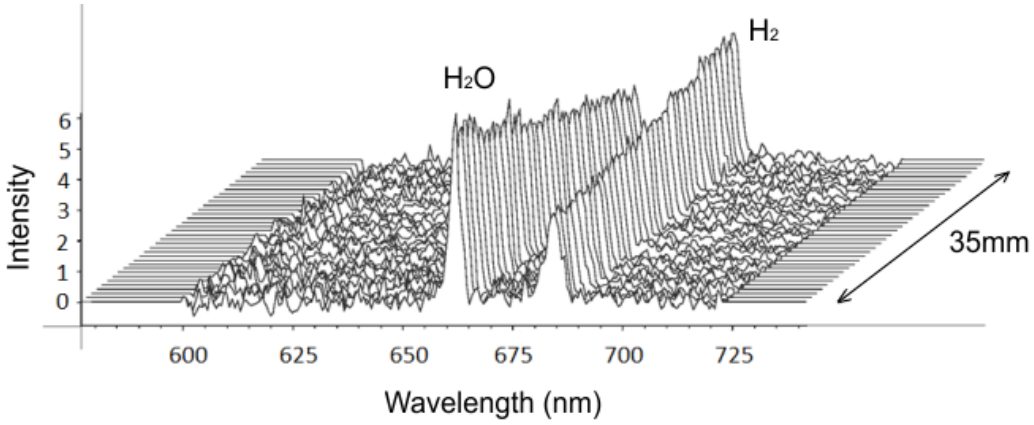

Fig. 11: Raman spectra recorded during operation of the SOFC with hydrogen. The 35 spectra cover a length of 35 mm and have been averaged over 3000 laser shots. The H_2O Raman band appears at $\lambda \approx 660$ nm and the H_2 Raman band at $\lambda \approx 683$ nm.

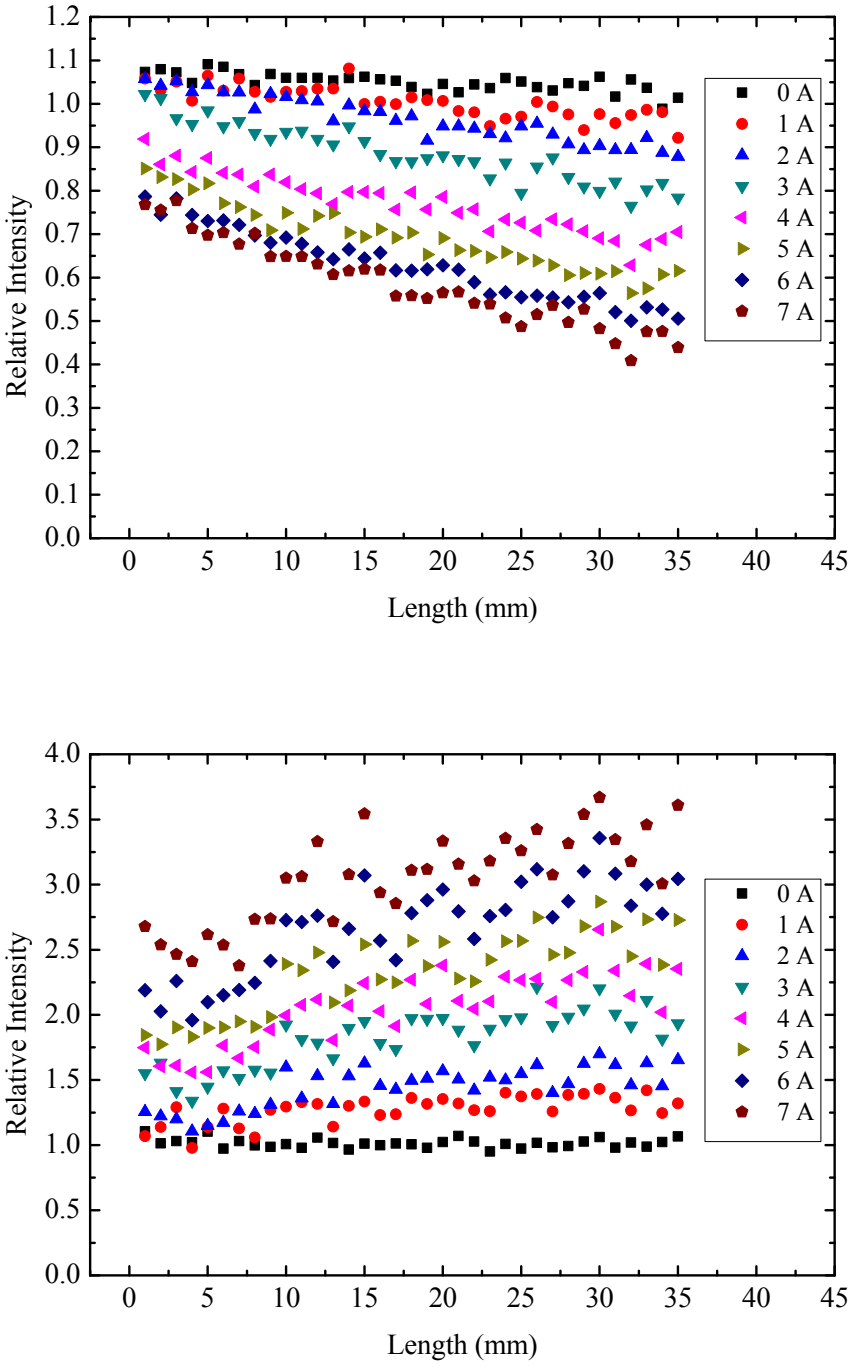

Fig. 12: In-situ measurements of H_2 (upper diagram) and H_2O (lower diagram) concentrations along the anode flow channel during operation of the SOFC at 1123 K at different cell currents.